EVA implants for controlled drug delivery to the inner ear

Y. Bedulho das Lages, N. Milanino, J. Verin, Jean-François Willart, Florence Danede, C. Vincent, P. Bawuah, J.A. Zeitler, F. Siepmann, J. Siepmann

International Journal of Pharmaceutics: X 8 (2024) 100271

Contents lists available at ScienceDirect

International Journal of Pharmaceutics: X

journal homepage: www.sciencedirect.com/journal/international-journal-of-pharmaceutics-x

EVA implants for controlled drug delivery to the inner ear

Y. Bedulho das Lages [a], N. Milanino [a], J. Verin [a], J.F. Willart [b], F. Danede [b], C. Vincent [a], P. Bawuah [c], J.A. Zeitler [c], F. Siepmann [a], J. Siepmann [a,*]

[a] Univ. Lille, Inserm, CHU Lille, U1008, F-59000 Lille, France
[b] Univ. Lille, UMR CNRS 8207, UMET, F-59000 Lille, France
[c] Univ. Cambridge, Department of Chemical Engineering and Biotechnology, Cambridge CB3 0AS, UK

ARTICLE INFO

Keywords:
Poly(ethylene vinyl acetate)
Dexamethasone
Inner ear
Hot melt extrusion
Controlled release

ABSTRACT

This study evaluated the potential of poly(ethylene vinyl acetate) (EVA) copolymers as matrix formers in miniaturised implants, allowing to achieve controlled drug delivery into the inner ear. Due to the blood-cochlea barrier, it is impossible to reliably deliver a drug to this tiny and highly sensitive organ in clinical practice. To overcome this bottleneck, different EVA implants were prepared by hot melt extrusion, altering the vinyl acetate content and implant diameter. Dexamethasone was incorporated as a drug with anti-inflammatory and anti-fibrotic activity. Its release was measured into artificial perilymph, and the systems were thoroughly characterised before and after exposure to the medium by optical and scanning electron microscopy, SEM-EDX analysis, DSC, X-ray powder diffraction, X-ray microtomography and texture analysis. Notably, the resulting drug release rates were much higher than from *silicone*-based implants of similar size. Furthermore, varying the vinyl acetate content allowed for adjusting the desired release patterns effectively: With decreasing vinyl acetate content, the crystallinity of the copolymer increased, and the release rate decreased. Interestingly, the drug was homogeneously distributed as tiny crystals throughout the polymeric matrices. Upon contact with aqueous fluids, water penetrates the implants and dissolves the drug, which subsequently diffuses out of the device. Importantly, no noteworthy system swelling or shrinking was observed for up to 10 months upon exposure to the release medium, irrespective of the EVA grade. Also, the mechanical properties of the implants can be expected to allow for administration into the inner ear of a patient, being neither too flexible nor too rigid.

1. Introduction

Treating diseases and disorders of the inner ear (also called cochlea) is highly challenging due to the "blood-cochlea barrier" (Juhn et al., 1982; Swan et al., 2008; El Kechai et al., 2015). The latter effectively protects this tiny and very sensitive organ, hindering the partitioning of drugs from the bloodstream into the inner ear. Thus, using conventional administration routes (e.g., i.v., i.m. or transdermal), the resulting drug concentrations at the target site are too low to allow for therapeutic effects. Direct drug injection into the perilymph (the primary liquid in the inner ear) might help overcome this obstacle. However, due to drug elimination from the target site, *repeated* administrations would be required. This is not possible in practice because each injection is invasive and associated with a non-negligible risk of infections and damage to the highly sensitive tissue. For these reasons, it is not yet possible to appropriately deliver a drug into the cochlea in clinical practice. This is unfortunate because a variety of highly potent drugs could potentially be used to treat widely spread diseases and disorders, such as hearing loss: The 2021 WHO report on hearing (World Health Organization, 2021) estimates that more than 1.5 billion people currently experience hearing loss. This number is expected to grow to 2.5 billion in 2050. More than 400 million people (including 34 million children) are estimated to suffer from *disabling* hearing loss, substantially affecting their health and quality of life. This number will likely grow to 700 million in 2050. Also, the financial loss to our societies is estimated at 1 trillion US $ each year (World Health Organization, 2021).

Different strategies have been proposed to overcome this critical obstacle and enable drug delivery to the cochlea, including administering dosage forms into the *middle* ear and miniaturised implants inserted directly into the *inner* ear (El Kechai et al., 2016; Lehner et al., 2019; Gausterer et al., 2020; Lehner et al., 2021; Mäder et al., 2018;

* Corresponding author at: University of Lille, College of Pharmacy, INSERM U1008, 3, rue du Professeur Laguesse, 59006 Lille, France.
E-mail address: juergen.siepmann@univ-lille.fr (J. Siepmann).

https://doi.org/10.1016/j.ijpx.2024.100271
Received 24 June 2024; Received in revised form 27 July 2024; Accepted 29 July 2024
Available online 31 July 2024

Jaudoin et al., 2021a; Jaudoin et al., 2021b; Lehner et al., 2022). Upon administration into the *middle* ear, the drug must first be released and subsequently diffuse through the round or oval window to reach its target site. Unfortunately, the residence time of many formulations at the administration site is unreliable because more or less liquid can be present in the middle ear, eliminating, for instance, a gel formulation. *Intracochlear* administration is more reliable but more invasive. Ideally, one single administration is sufficient to limit the risk of infections and tissue damage. Different types of *miniaturised* implants have been proposed for such a direct insertion into the inner ear (Toulemonde et al., 2022; Hügl et al., 2019; Liu et al., 2015; Liu et al., 2016). Frequently, silicone is used as the matrix-forming polymer in these cases (Qnouch et al., 2021; Rongthong et al., 2022; Gehrke et al., 2016a). The drug is embedded into the silicone. Upon contact with perilymph, water penetrates into the implant, and the drug dissolves & diffuses out of the device. However, the resulting drug release rates are generally very low (Krenzlin et al., 2012; Gehrke et al., 2019). Attempts to increase the permeability of silicones to accelerate drug release showed limited success: Complete drug release often still requires many years (Gehrke et al., 2016b). This type of slow, very long-term drug delivery is not optimal for all types of drugs and diseases/disorders. Thus, there is a clinical need for faster drug release kinetics from intracochlear implants.

Poly(ethylene vinyl acetate) (EVA) is an interesting copolymer, which has been used as matrix former and film coating material in various controlled drug delivery systems (Genina et al., 2016; Moroni et al., 2023; Chen et al., 2022). A comprehensive review of Schneider et al. (Schneider et al., 2017) gives a good overview on possible applications, including vaginal rings (Novák et al., 2003; Gruber, 2006), intrauterine implants (Salem and Baskin, 1993), subcutaneous implants (Croxatto, 2000; Mansour, 2010; Le and Tsourounis, 2001), ocular systems (Kuno and Fujii, 2011; Bourges et al., 2006) and stents (Guo et al., 2007). EVA is a thermoplastic copolymer built of ethylene and vinyl acetate monomers. Polyethylene segments tend to crystallise: Theoretically, "EVA with zero vinyl acetate content" would be "low-density polyethylene" with about 50–60% crystallinity (Brogly et al., 1997; Salyer and Kenyon, 1971; Zhang et al., 2002). The presence of vinyl acetate units sterically hinders the crystallisation of the polyethylene segments. Thus, with increasing vinyl acetate content, the crystallinity of the copolymer decreases. EVA grades with a vinyl acetate content of 40% and more are considered amorphous (Brogly et al., 1997; Zhang et al., 2002). Interestingly, the group of Henry Brem at Johns Hopkins University incorporated dexamethasone into EVA matrices for treating oedema in the brain (Reinhard et al., 1991). They prepared cylindrical discs by solvent evaporation: The copolymer was dissolved in methylene chloride, the drug was added, and the liquid was cast into cylindrical moulds (5 mm diameter), frozen and the solvent evaporated under vacuum. Following intracranial implantation in rats, dexamethasone was detected in the brain tissue for up to 21 d. Appropriately purified EVA (e.g. after elimination of catalysts) is considered to be non-toxic and biocompatible. Several EVA-based controlled drug delivery systems for parenteral application are available on the market (Schneider et al., 2017). Since EVA is non-degradable, empty remnants might either be removed upon complete drug release or remain in the patient's body.

Different types of mass transport phenomena can be involved in the control of drug release from a polymeric matrix system, including for example water diffusion into the device, plasticising effects of water on the polymer (Blasi et al., 2005), drug dissolution (Siepmann and Siepmann, 2013), the diffusion of dissolved drug molecules and/or ions due to concentration gradients (Fredenberg et al., 2011; Siepmann and Siepmann, 2012), saturation effects within the dosage form and/or within the surrounding environment (Siepmann and Siepmann, 2020), system swelling (Bode et al., 2019), polymer degradation (von Burkersroda et al., 2002), the potential creation of acidic microclimates due to degradation products (Schädlich et al., 2014), osmotic effects (Brunner et al., 1999) and drug degradation. To better understand which mass transport phenomena play an important role in a *specific* drug delivery system, the latter should be thoroughly physico-chemically characterised before and after exposure to the release medium. If possible, non-invasive characterisation methods like X-ray microtomography should be preferred.

This study aimed to evaluate the potential of EVA copolymers as matrix formers in miniaturised implants, enabling reliable drug delivery to the inner ear at much higher rates than silicone-based systems (Rongthong et al., 2022; Gehrke et al., 2016a; Krenzlin et al., 2012; Gehrke et al., 2019). Dexamethasone was incorporated as a drug because of its anti-inflammatory and anti-fibrotic activity (Wilk et al., 2016; Farhadi et al., 2013; Gao et al., 2021). In addition, in the case of hearing loss, long-term exposure to dexamethasone can be expected to prolong the lifetime expectancy of remaining hair cells (playing a crucial role in hearing). The implants were prepared by hot melt extrusion. The vinyl acetate content varied from 15 to 40%, and the implants' diameter from 0.5 to 1 mm. Dexamethasone release was measured into artificial perilymph at 37 °C. The implants were thoroughly characterised before and after exposure to the release medium, using optical and scanning electron microscopy, SEM-EDX analysis, DSC, X-ray powder diffraction, X-ray microtomography and texture analysis.

2. Materials and methods

2.1. Materials

Dexamethasone (Discovery Fine Chemicals, Dorset, UK); 3 grades of poly (ethylene vinyl acetate) (EVA): Elvax 40 W, Elvax 260 A and Elvax 550 A, with a vinyl acetate content of 40, 28 and 15% *w/w* (EVA 40, EVA 28 and EVA 15) (oval granules; DuPont, Geneva, Switzerland); acetonitrile and methanol (HPLC grade; Carlo Erba Reagents, Val De Reuil, France); acetone and ethanol (VWR Chemicals, Fontenay-sous-Bois, France); isopropanol (99.5% for HPLC, Acros Organics, Geel, Belgium); ethyl acetate (HPLC grade, Fisher, Loughborough, UK); ultrapure water (Purelab flex; Veolia Water Technologies, Aubervilliers, France); calcium chloride dihydrate, magnesium sulphate monohydrate, potassium chloride, and HEPES Pufferan (Carl Roth, Karlsruhe, Germany); sodium chloride (Cooper, Melun, France).

2.2. Implant preparation

EVA granules and dexamethasone powder (both used as received) were manually blended with a pestle in a mortar for 10 min. The blends were hot melt extruded using a Leistritz "Nano 16" apparatus (4 heating zones; Leistritz, Nuremberg, Germany), equipped with a co-rotating twin screw (16 mm diameter). The diameter of the circular die orifice was 0.3, 0.7 or 4 mm, as indicated. The screw speed and feed rate were kept constant at 30 rpm and 3 cm^3/min, respectively. The processing temperatures were adapted to the melting points of the investigated EVA grades as follows: *EVA 40:* 45 °C, 80–85–90-80 °C; *EVA 28:* 80 °C, 110–115–120-110; *EVA 15:* 90 °C, 125–125–125-125 °C (melting point, temperature of the die - zone 1 - zone 2 - zone 3). The screw configuration is shown in Fig. S1. The extrudates were air-cooled and manually cut into cylinders.

2.3. Determination of the practical drug loading

About 5 mg extrudate samples were exposed to 10 mL acetone in a test tube at room temperature for 4 h (hourly vortexing for 15 s). The liquid was completely renewed, and the samples incubated for another 20 h in fresh acetone (vortexing after 4 and 20 h for 15 s). The bulk fluids were filtered (PVDF syringe filters, 0.45 µm; Agilent Technologies, Santa Clara, USA), and their drug content was measured by HPLC-UV analysis as follows: An Alliance e2695 apparatus (Waters Division, Milford, USA), equipped with a UV detector, was used. Samples (20 µL) were injected into a reverse phase column C18 (Gemini 3 µm, 110 Å, 100 ×

4.6 mm; Phenomenex, Le Pecq, France), which was kept at 25 °C. The mobile phase was an acetonitrile: water 33:67 V:V blend. The flow rate was set to 1.2 mL/min. The detection wavelength was 254 nm, and the retention time was about 5 min. Each experiment was performed in triplicate. Mean values +/− standard deviations are reported.

2.4. Drug release measurements

Implants with a diameter of *0.3 mm* were placed into vials or Eppendorf tubes (1 implant per vial or tube), filled with 200 or 800 µL artificial perilymph (as indicated). Implants with a diameter of *0.7 mm* were placed into Eppendorf tubes (1 implant per tube), filled with 2.8 mL artificial perilymph. The latter was an aqueous solution of 1.2 mM calcium chloride dihydrate, 2.78 mM magnesium sulphate monohydrate, 2.7 mM potassium chloride, 5 mM HEPES Pufferan and 145 mM sodium chloride. The vials or tubes were placed in a horizontal shaker (80 rpm, GFL 3033; Gesellschaft fuer Labortechnik, Burgwedel, Germany) and kept at 37 °C. The release medium was completely withdrawn and replaced by fresh bulk fluid at predetermined points. The withdrawn samples were filtered, and their drug concentrations were measured by HPLC-UV analysis, as described in *section 2.3*. Sink conditions were maintained throughout the experiments. Each experiment was performed in triplicate. Mean values +/− standard deviations are reported.

2.5. Optical microscopy

Optical microscopy pictures of EVA granules and implants were taken before and after exposure to artificial perilymph (as indicated), using an Axiovision Zeiss Scope-A1 microscope, equipped with an AxioCam ICc1 camera and the Axiovision Zeiss Software (Carl Zeiss, Jena, Germany).

2.6. SEM and SEM-EDX analyses

Implant samples were analysed by SEM using a Jeol Field Emission Scanning Electron microscope (JSM-7800F, Tokyo, Japan). Radial and longitudinal cross-sections were obtained by manual cutting with a scalpel. Samples were fixed with a ribbon carbon double-sided adhesive on the sample holder and covered with a fine carbon layer. Optionally, SEM imaging was coupled with Energy-dispersive X-ray microanalysis (EDX analysis, X-Max SDD detector, Aztec 3.3 software; Oxford Instruments, Oxford shire, UK). The presence of carbon, nitrogen, oxygen, fluorine, and chlorine was observed at 5 keV.

2.7. DSC and mDSC measurements

Differential Scanning Calorimetry (DSC) thermograms of the raw materials and implants were recorded using a DCS1 Star System (Mettler Toledo, Greifensee, Switzerland). Approximately 5 mg raw material/10 mg implant samples were heated in perforated aluminium pans as follows: holding for 5 min at −60 °C, followed by heating at 10 °C/min to 300 °C.

mDSC thermograms were recorded using a TA Instruments Q1000 calorimeter (TA Instruments, Leatherhead, UK). The chamber was purged with dry nitrogen at a 50 mL/min flow rate. Indium was used for temperature and enthalpy calibration. The heat capacity calibration was performed at 96.9 °C using sapphire disks. About 2–4 mg samples were analysed in open aluminium pans (TA Instruments). They were heated from −80 to 170 °C at 5 °C/min, with a modulation of ±0.663 °C and a period of 50 s. Glass transition temperatures (Tgs) were determined from the reverse heat flow signal using the Universal Analysis 2000 software (TA Instruments).

2.8. Thermogravimetric analysis (TGA)

Thermogravimetric analyses were performed with a Q500 TGA from TA Instruments (Guyancourt, France). Samples were placed in open aluminium pans, and the furnace was flushed with highly pure nitrogen (50 mL/min). The temperature reading was calibrated using the Curie points of alumel and nickel, while the mass reading was calibrated using balance tare weights provided by TA Instruments. All TGA scans were performed at 5 °C/min.

2.9. X-ray powder diffraction analysis

X-ray powder diffraction patterns were recorded using a PANalytical X'Pert pro MPD powder diffractometer (PANalytical, Almelo, Netherlands), equipped with a Cu X-ray tube ($\lambda CuK\alpha = 1.54$ Å) and the X'celerator detector. Samples were placed in a spinning flat sample holder. The measurements were performed in Bragg–Brentano θ-θ geometry. The diffractograms were recorded from 3 to 60° (2θ) (0.0167° steps, 100 s/step).

2.10. X-ray microtomography (X-ray µCT)

EVA granules (as received), dexamethasone-loaded, and drug-free implants were characterised by X-ray microtomography (Skyscan 1172, Bruker microCT, Kontich, Belgium), applying a source voltage of 35 kV. The samples were rotated during the measurements, and 1440 transmission images were recorded in steps of 0.25°. The exposure time for each transmission image was 780 ms. The scan duration for one sample was 1 h 59 min. Reconstruction of the µCT images was performed with the NRecon software (ver. 1.6.8, Bruker microCT, Kontich, Belgium). Further image analysis was conducted with the Dataviewer software (ver. 1.5.2, Bruker microCT, Kontich, Belgium). The isotropic voxel size of the reconstructed images varied between 2.24 and 2.26 µm. If indicated, the implants had been exposed to artificial perilymph prior to the measurements as described in *Section 2.4* and subsequently dried in an oven at 37 °C for 48 h.

2.11. Tensile testing

The tensile test was carried out with a TA.XT plus Texture Analyzer (Stable Micro Systems, Godalming, UK), equipped with a 5 kg load cell and a tensile probe (Mini Tensile Grips, part code A/MTG). The experimental conditions were as follows: 30 mm clamp distance, tension test mode, 1.0 mm/s pre-test speed, 2 mm/s strain rate, 10 mm/s post-test speed, strain target mode, 10,000 g target force, auto (force) trigger mode, 200.0 g trigger force, level break mode, 200.0 g break sensitivity, stop upon break detect. Data were collected and processed using the Exponent Connect software (Stable Micro Systems). The Young modulus was determined as the slope of the linear portions of the strain-stress plots (0–10% strain). Each experiment was performed six times. Mean values +/− standard deviations are reported.

3. Results and discussion

This study aimed to prepare miniaturised EVA-based implants and evaluate their potential to enable controlled drug delivery to the inner ear. Dexamethasone (13% loading) was incorporated as the drug. Three EVA grades were investigated, differing in their vinyl acetate content (40, 28, 15%, *w*/w): EVA 40, 28 and 15, respectively. The implants were prepared by hot melt extrusion (diameter of the circular orifice: 0.3, 0.7 and 4 mm), adapting the processing temperatures to the melting points of the EVA grade: *EVA 40* 80–85–90-80 °C; *EVA 28*110–115–120-110 °C; *EVA 15*125–125–125-125 °C (temperature of the die - zone 1 - zone 2 - zone 3). The extrudates were manually cut into cylinders. Notably, the TGA thermograms of all EVA grades did not show any mass loss in these temperature ranges. As illustrated in Fig. S2, the samples' mass

remained constant up to about 250 °C. Furthermore, dexamethasone is known to be stable at the temperatures used for hot melt extrusion in this study. The melting point of the drug powder raw material was determined to be approximately 266 °C by DSC analysis (Fig. S3).

3.1. Implant properties before exposure to the release medium

Optical microscopy pictures of *drug-free* implants based on EVA 40, EVA 28 and EVA 15 before exposure to the release medium are shown on the left-hand side of Fig. 1. As can be seen, the systems were transparent, irrespective of the EVA grade. In contrast, all dexamethasone-loaded implants were opaque (right-hand side in Fig. 1). This can serve as a first indication that the dexamethasone is likely distributed as *solid particles* throughout the macromolecular networks and not as individual molecules (dissolved) (or at least, not all of the drug was dissolved). All implants (drug-free and drug-loaded) had a relatively homogeneous appearance, irrespective of the EVA grade. Please note that the surface of EVA 15-based implants was shrivelled under the selected processing conditions. However, smooth surfaces can likely be obtained at different extrusion rates (it was beyond the scope of this study to optimise this aspect). Note that the diameter of the implants was greater than the diameter of the orifice. This is because the cylindrical filaments leaving the hot melt extruder rapidly expanded. Importantly, a diameter of 0.5 mm is compatible with an administration into a human cochlea.

Figure 2 shows SEM pictures of surfaces and cross-sections of drug-loaded implants based on: A) EVA 40, B) EVA 28, and C) EVA 15 before exposure to the release medium. Cross-sections were observed at different degrees of magnification. Clearly, the surfaces were non-porous and relatively smooth, irrespective of the EVA grade. Cross-sections revealed the presence of tiny particles distributed throughout the systems. EDX analysis allowed to identify them as dexamethasone particles: At the top of Fig. 3, EDX spectra and an SEM picture of a cross-section of an EVA 40 implant (before exposure to the release medium) are illustrated. The EDX spectra correspond to the two zones highlighted in the SEM picture. Importantly, fluorine is only present in dexamethasone, not in EVA. Thus, its presence allows distinguishing between

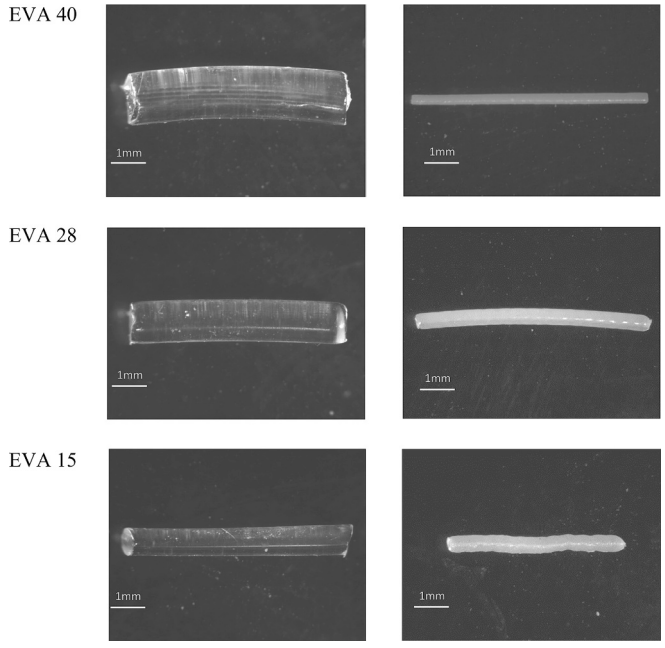

Fig. 1. Optical microscopy pictures of drug-free and dexamethasone-loaded implants based on EVA 40, EVA 28 and EVA 15 before exposure to artificial perilymph. Please note that differences in the diameters can be attributed to different pulling speeds of the filaments during production. The diameter of the circular orifice was 0.3 mm.

these two compounds. As can be seen, the zone located in the particle in the middle of the SEM picture is relatively rich in fluorine, indicating the presence of dexamethasone. In contrast, the other highlighted zone is relatively poor in fluorine. Thus, it essentially is drug-free. Importantly, the cross-sections of all EVA implants showed a homogeneous distribution of dexamethasone particles throughout the systems, irrespective of the EVA grade (Fig. 2). Please note that the SEM cross-sections also show multiple holes. However, most can be expected to be artefacts: Drug crystals likely fell out of the implants during sample cutting. As explained in the following, *non-destructive* X-ray μCT measurements did not show evidence of numerous empty holes in the implants before exposure to the release medium.

X-ray diffraction analysis revealed that the tiny dexamethasone particles distributed throughout the EVA implants were in a *crystalline* state. Fig. 4 shows the X-ray diffraction patterns of drug-loaded implants, based on: A) EVA 40, B) EVA 28 and C) EVA 15. The implant diameter was 0.5 or 1.0 mm, as indicated. The X-ray diffraction patterns of the raw materials (dexamethasone powder and EVA granules, as received) and drug-free implants are illustrated for comparison. The raw material of dexamethasone was crystalline, corresponding to the polymorphic Form A described by Oliveira et al. (Oliveira et al., 2018). Characteristic peaks of this form (e.g., at 2 Θ = 13.5 or 16°) were also observed in all drug-loaded EVA implants, irrespective of the EVA grade. In contrast, EVA 40 granules and drug-free implants based on EVA 40 were X-ray amorphous (Fig. 4A). Note that EVA 28 and EVA 15 granules and the respective drug-free implants were *semi-crystalline*, exhibiting diffraction peaks, for instance, at 2 Θ = 21°. This is due to crystalline regions in these EVA grades, formed by polyethylene chain segments (Schneider et al., 2017; Arsac et al., 2000). EVA 40 is X-ray amorphous because the presence of the vinyl acetate groups sterically hinders the crystallisation of polyethylene chain segments (Johnsen and Nachtrab, 1969). Importantly, manufacturing the implants by hot melt extrusion does not seem to alter the drug's or polymers' physical states under the given conditions.

DSC studies confirmed these hypotheses: Fig. 5 shows the thermograms of dexamethasone-loaded implants based on: A) EVA 40, B) EVA 28 and C) EVA 15 before exposure to the release medium. The diameter was 0.5 or 1.0 mm, as indicated. The DSC thermograms of the EVA raw materials (granules) and drug-free implants are shown for comparison. Notably, most of the drug-loaded implants showed an endothermic peak in the vicinity of the melting temperature of the crystalline dexamethasone raw material (Fig. S3), irrespective of the EVA grade and implant diameter (marked by the *black* flashes in Fig. 5). However, in two cases (EVA 40 implants with a diameter of 1.0 mm and EVA 15 implants with a diameter of 0.5 mm), this endothermic event seemed to be shifted to lower temperatures (marked by *orange* flashes). This might be explained by the dissolution of the crystalline dexamethasone particles in the melted polymers during the DSC analysis before reaching the melting temperature of the drug. It is unclear why this phenomenon was not observed in all cases. It was beyond the scope of this study to investigate this phenomenon in more detail.

In all EVA samples, two endothermic events were observed below 100 °C (Fig. 5), likely corresponding to two melting events of crystalline regions in these polymers: Arsac et al. (Arsac et al., 2000) reported two melting temperatures for EVA with 40, 28, and 14% vinyl acetate content (38.4 & 55.5 °C, 45.5 & 73.5 °C, and 49 & 90 °C, respectively). They hypothesised that this behaviour indicates a *not completely randomised distribution of the monomers in macromolecular chains*. Instead, EVAs are likely slightly sequenced copolymers. Wang et al. (Wang et al., 2006) also reported two large endothermic peaks in EVA samples in this temperature range, corresponding to the melting of two different crystalline species. Please note that in the case of EVA 40, the raw material was likely amorphous (please see above). However, upon heating during the DSC measurements parts of the material likely crystallised (which is consistent with small exothermic peaks that were observed prior to melting). Furthermore, Baker et al. (Baker, 1987) reported a glass

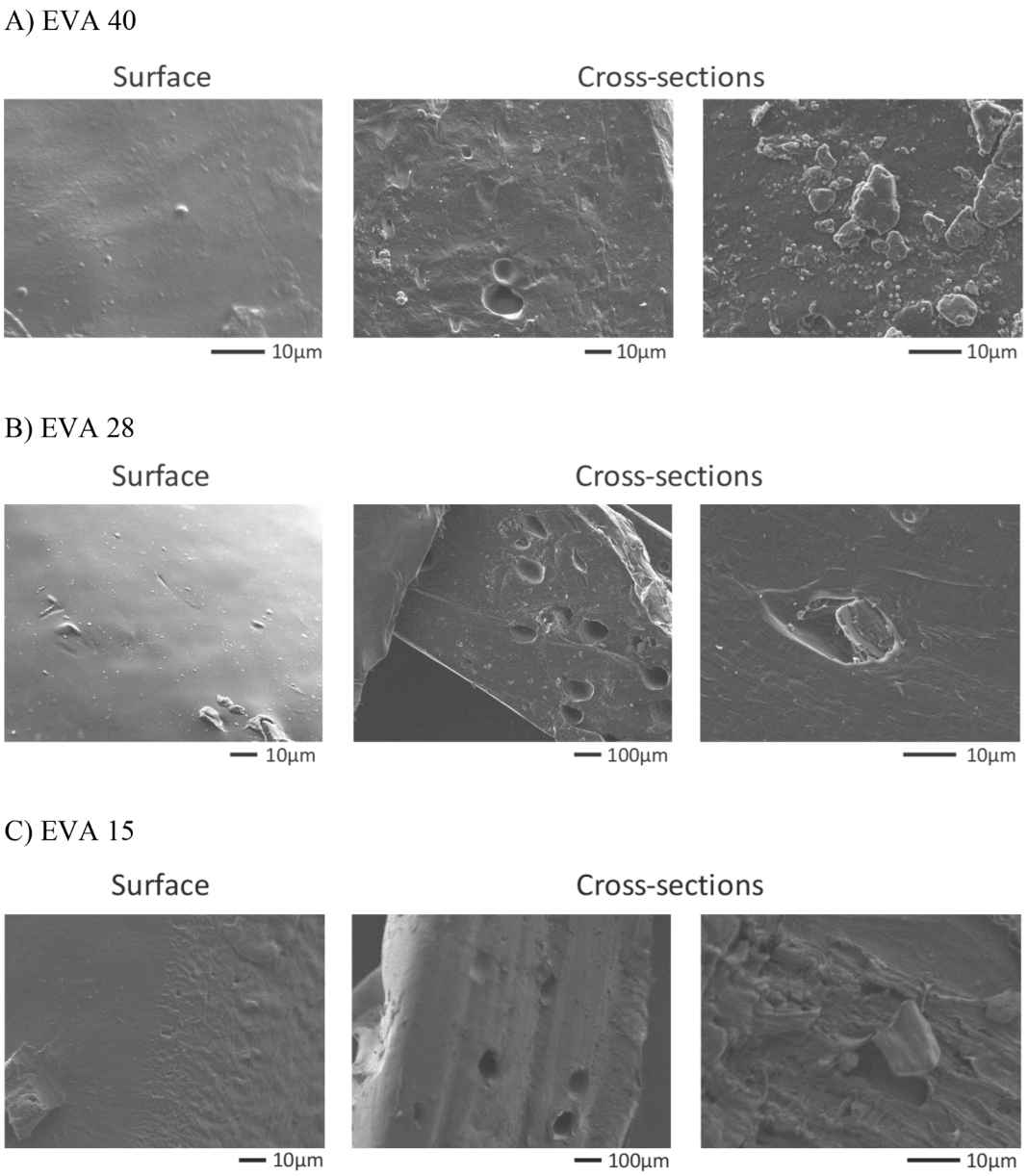

Fig. 2. SEM pictures of surfaces and cross-sections of dexamethasone-loaded implants before exposure to artificial perilymph, based on: A) EVA 40, B) EVA 28, and C) EVA 15.

transition temperature (Tg) of about −25 °C for EVA grades with a vinyl acetate content of up to 50%. mDSC thermograms recorded with the EVA raw materials used in this study also revealed a Tg of about −25 °C (mid-points, Fig. S4).

To monitor the inner structure of the *entire* implants in a *non-destructive* manner (and not only of specific regions, which were cross-sectioned), X-Ray µCT was applied. EVA implants were analysed before and after exposure to the release medium. The polymer raw material (oval EVA granules) was also studied for comparison. The picture at the top of Fig. 6 shows an example of a *virtual* cross-section through half an EVA 40 granule (the granule was cut in half to fit into the sample holder of the apparatus). As can be seen, the inner structure appears to be dense (non-porous) and homogeneous. Video 1 shows a series of virtual cross-sections through the half granule, starting from the bottom of the sample and going along the z-axis to its top (illustrated in the scheme in Fig. 6). The entire EVA granule appears to be dense and homogeneous.

Virtual X-ray µCT cross-sections through a *dexamethasone-loaded implant* based on EVA 40 before exposure to the release medium are shown at the top of Fig. 7. The cross-sections were made in different planes, as illustrated in the cartoons at the bottom. Importantly, all pictures confirm a homogeneous distribution of numerous tiny drug particles throughout the implants, irrespective of the plane of the cross-section. They appear as *bright grey* dots (note that the occasionally observed *white* spots -especially at the systems' surface- are artefacts). Video 2 shows a series of virtual cross-sections through the implant along the z-axis, starting from the bottom of the cylinder and going to its top (the cartoon at the bottom of Fig. 7 shows the coordinate system and implant). As seen in the video, dexamethasone is distributed in the form of tiny particles in a homogeneous manner throughout the *entire* EVA implant. Also, virtually no empty holes are visible, indicating that most of the cavities observed in Fig. 2 (SEM pictures of cross-sections) were artefacts generated during sample cutting.

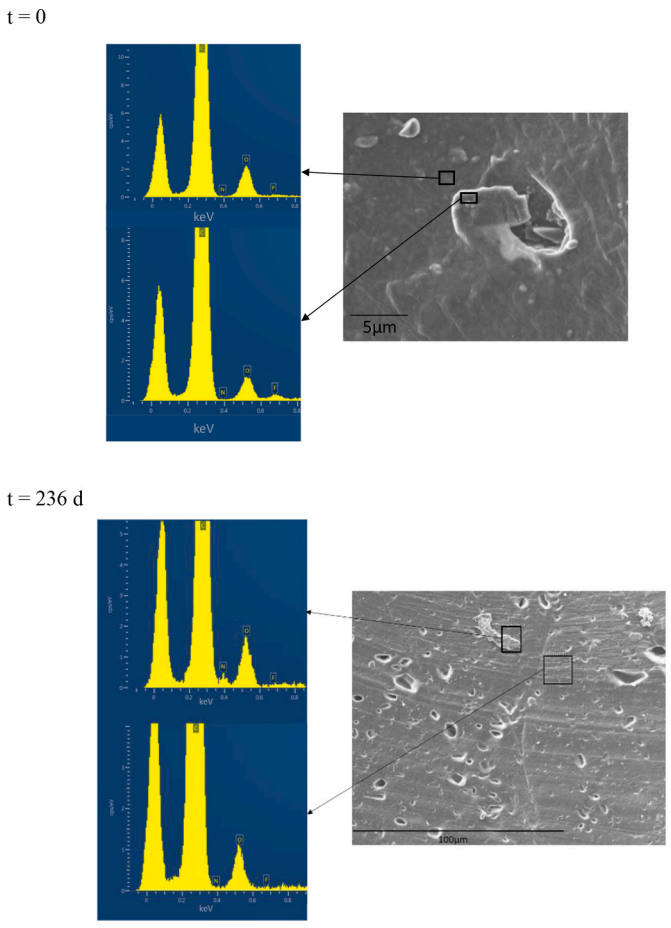

Fig. 3. EDX spectra and SEM pictures of cross-sections of dexamethasone-loaded EVA 40 implants before and after 263 d exposure to the release medium. The EDX spectra correspond to the zones highlighted in the SEM pictures.

3.2. Dexamethasone release kinetics

Figure 8 shows the release kinetics of dexamethasone from the investigated EVA implants into artificial perilymph at 37 °C. The initial implant diameter and volume of the bulk fluid were: A) 0.5 mm and 200 µL, B) 0.5 mm and 800 µL, and C) 1.0 mm and 2.8 mL. Figs. 8A and B show drug release from the same type of implants but in different volumes of release medium. Fig. 8B and C illustrate dexamethasone release from thinner and thicker implants, respectively, keeping the ratio "implant volume: bulk fluid volume" constant. The grey, orange and blue curves correspond to systems based on EVA 40, 28 and 15, respectively. In all cases, sink conditions were provided throughout the experiments.

As can be seen, the EVA grade and implant diameter substantially affected drug release. In contrast, the volume of the release medium had virtually no impact under the given conditions (comparing Fig. 8A vs. 8B or looking at Fig. S5, showing a direct comparison of the respective release curves in one diagram). This indicates that the *implant* controls the release of the drug and not the surrounding bulk fluid (at least in the absence of saturation effects in the latter). Notably, the dexamethasone release rate significantly decreased with decreasing vinyl acetate content (40, 28, 15%, *w*/w), irrespective of the implant's diameter and volume of the release medium. This can be explained by the increasing crystallinity of the polymer with decreasing vinyl acetate content (as discussed above): The mobility of the polymer chains (and, thus, also of the drug molecules) is much lower in crystalline regions compared to amorphous zones. Hence, with decreasing vinyl acetate content, drug mobility decreases, resulting in slower dexamethasone release. From a practical point of view, this is very important and provides high flexibility in possible drug release rates: Varying the vinyl acetate content allows the release rate of a given drug to be adjusted effectively. It has to be pointed out that the drug release rates observed for dexamethasone in this study are substantially higher compared to miniaturised *silicone*-based implants reported in the literature (Rongthong et al., 2022; Gehrke et al., 2016a; Krenzlin et al., 2012; Gehrke et al., 2019). This difference can be of great clinical importance.

Note that an increase in the vinyl acetate content in EVA polymers

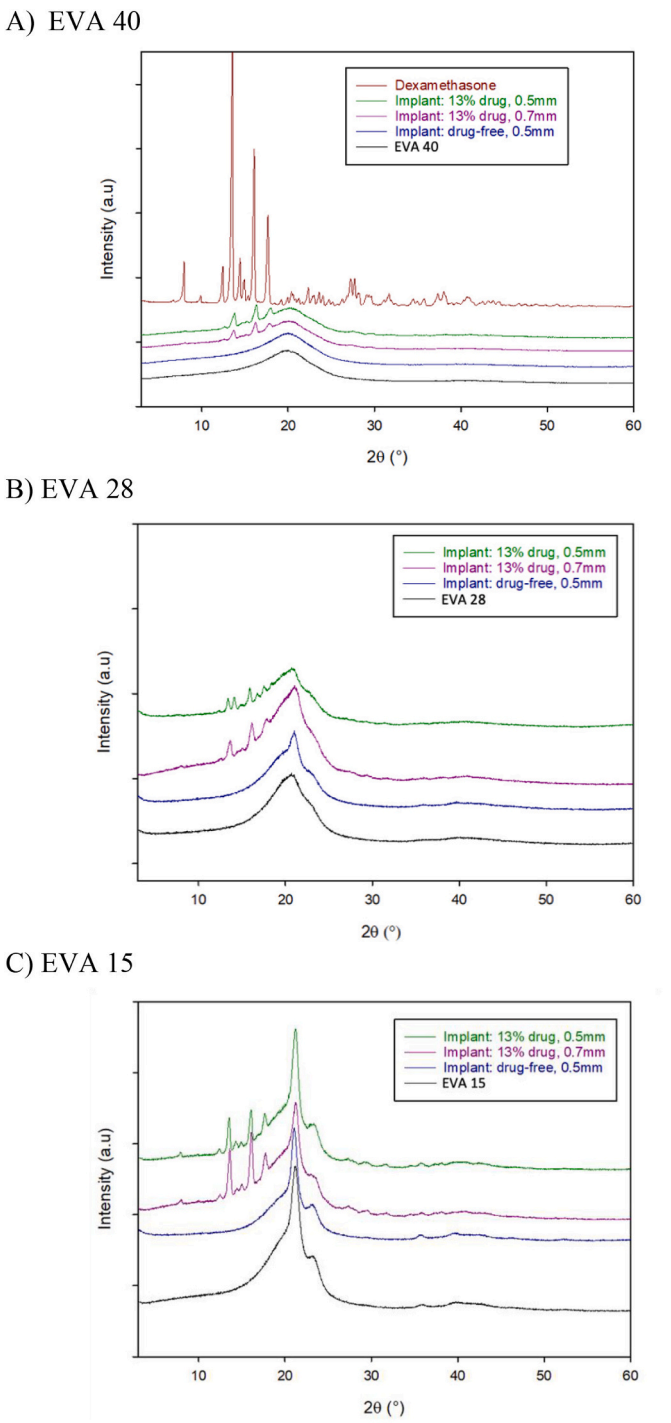

Fig. 4. X-ray diffraction patterns of drug-free and dexamethasone-loaded implants before exposure to artificial perilymph, based on: A) EVA 40, B) EVA 28, and C) EVA 15. The X-ray diffraction patterns of the raw materials (dexamethasone powder and EVA granules) are also shown for comparison.

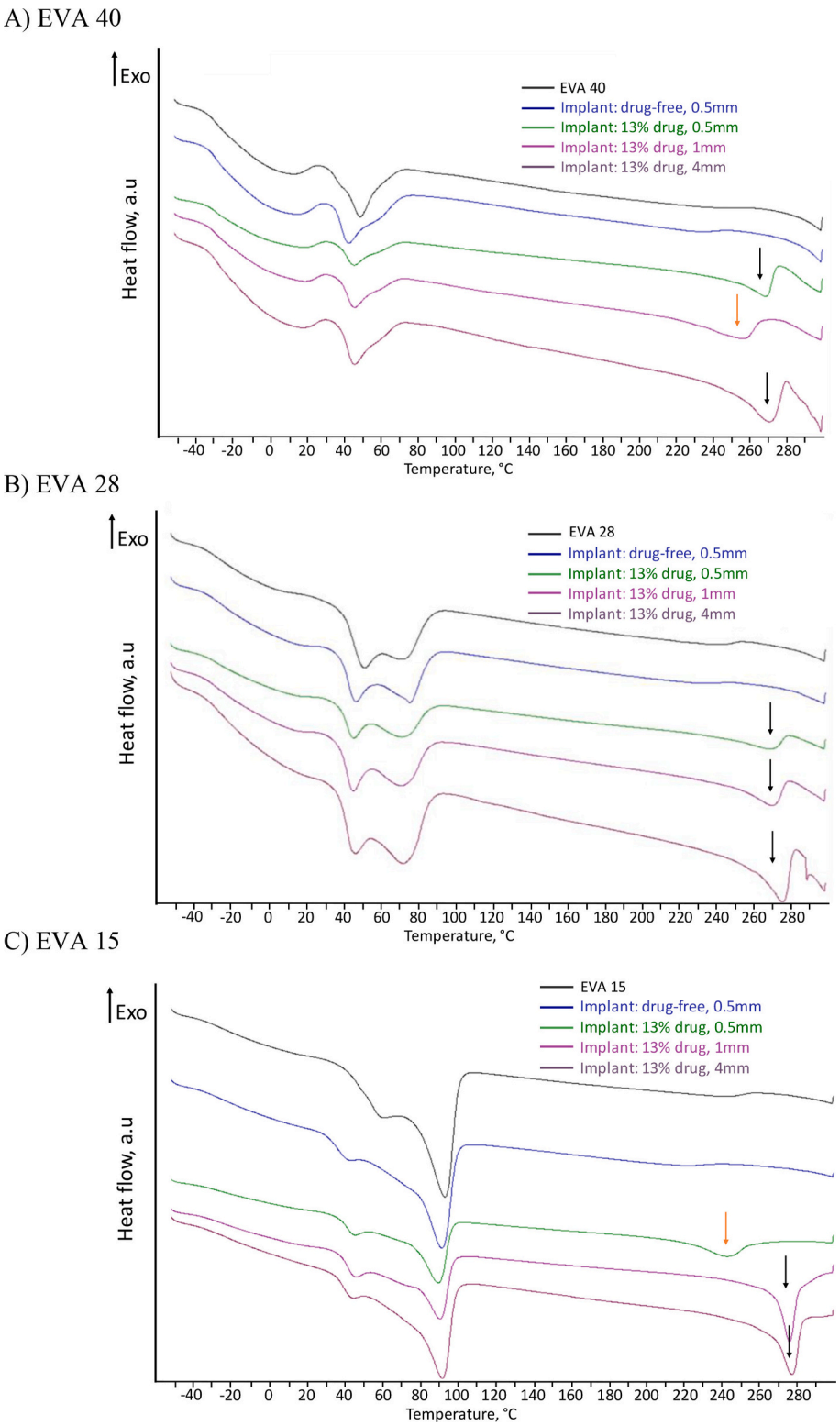

Fig. 5. DSC thermograms of drug-free and dexamethasone-loaded implants before exposure to artificial perilymph, based on: A) EVA 40, B) EVA 28, and C) EVA 15. The DSC thermograms of the EVA raw materials (granules) are shown for comparison. Black flashes indicate the melting of crystalline dexamethasone particles. Orange flashes likely indicate the dissolution of crystalline dexamethasone particles in melted EVA.

has also been reported to increase the system's glass transition temperature (Tg) (Baker, 1987). Since the mobility of the macromolecules is much higher in rubbery regions than in glassy zones, this can be expected to decrease drug mobility and, hence, the resulting drug release rate. However, up to a vinyl acetate content of approximately 50%, the Tg has been reported to remain about constant (Baker, 1987), and most of the EVA grades used for controlled drug delivery applications exhibit vinyl acetate contents of 40% or less.

The observed decrease in the relative drug release rate with increasing implant *diameter* (Fig. 8B vs. 8C) can be explained by the

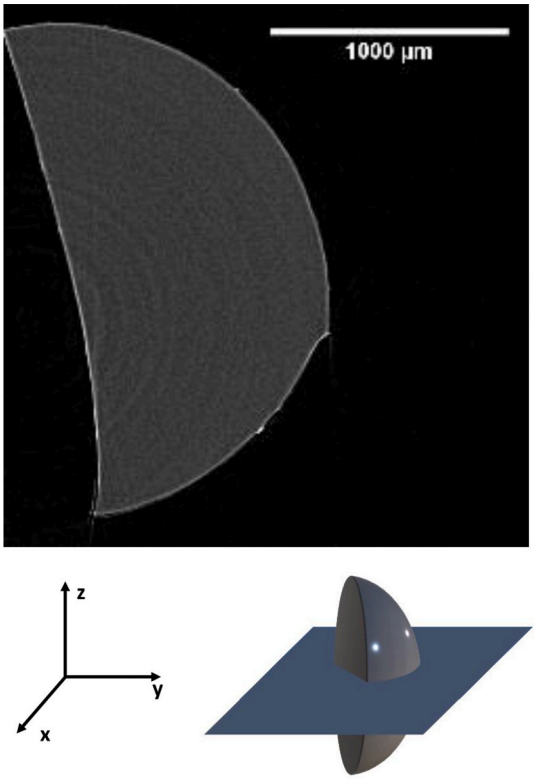

Fig. 6. X-ray µCT image of a virtual cross-section through half an EVA 40 granule (raw material). The cartoon shows the plane of the cross-section.

increasing lengths of the diffusion pathways to be overcome by the drug (Siepmann and Siepmann, 2012). Diffusional mass transport (Siepmann and Siepmann, 2013) can be expected to play a major role in EVA-based drug delivery systems. However, in the investigated implants, other phenomena might also play a significant role in the control of drug release, for instance, because dexamethasone is not freely soluble in aqueous media (e.g., 100 µg/mL in water at 25 °C) (O'Neil, 2001). Thus, in addition to diffusion, limited solubility effects *within* the polymeric matrix might be important (which should not be confused with potential saturation effects in *the surrounding bulk fluid* (Siepmann and Siepmann, 2020)).

The optical microscopy pictures in Fig. 9 show how the appearance of the investigated EVA implants changes during drug release. As seen in the case of EVA 40-based implants, surface-near regions become transparent first (Fig. S6 shows some of the pictures at a higher magnification). This indicates that the drug crystals located in these regions dissolve first. Once dissolved, the dexamethasone molecules diffuse out of the implants, due to concentration gradients. The drug "poor" EVA zones (free of non-dissolved dexamethasone particles) are transparent, as this is the case for drug-free implants (Fig. 1, left-hand side). Since dexamethasone release is slower from EVA 28- and EVA 15-based implants, this "drug depletion effect" of surface-near regions is not yet very pronounced in the pictures shown in Fig. 9 (zooms on some of the pictures are shown in Fig. S7).

The SEM picture at the bottom of Fig. 3 shows a cross-section through an EVA 40-based implant after 263 d exposure to the release medium. At this time point, dexamethasone release from the system was complete (Fig. 8). Numerous tiny holes can be seen throughout the polymeric matrix. They have likely been created upon the dissolution of the dexamethasone crystals during drug release. Note that the samples were dried for 48 h at 37 °C before analysis, so artefact creation cannot be excluded. The EDX spectra on the left-hand side at the bottom of Fig. 3 also do not show evidence for dexamethasone-rich regions. Furthermore, *virtual* X-ray µCT cross-sections through an EVA 40

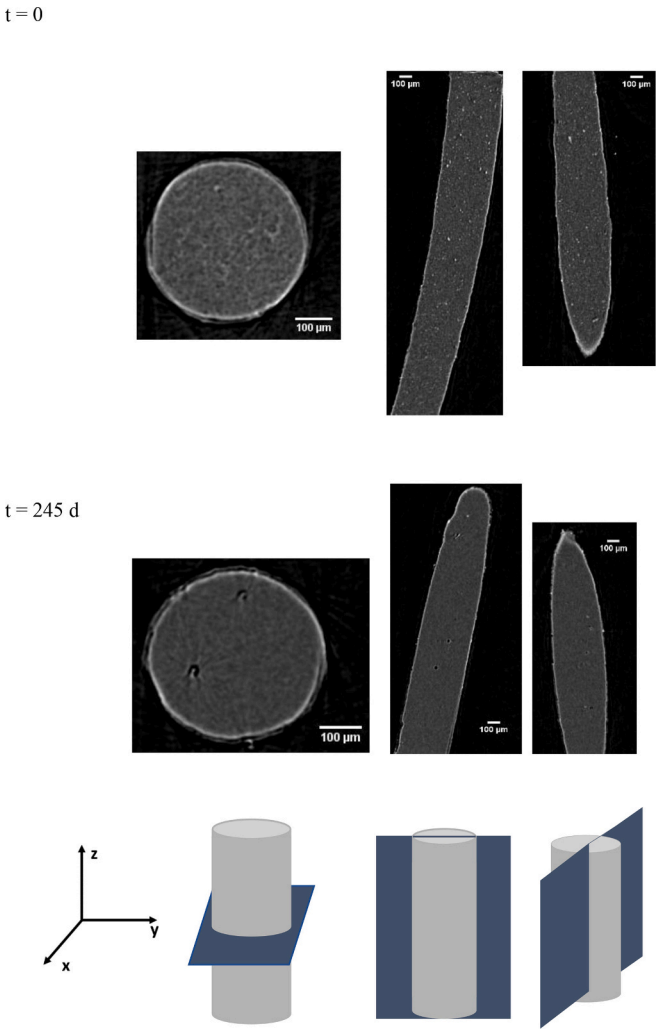

Fig. 7. X-ray µCT images of *virtual* cross-sections through a dexamethasone-loaded implant based on EVA 40 before and after 245 d exposure to artificial perilymph at 37 °C. After exposure to the release medium, the implant was dried for 48 h at 37 °C. The cartoons at the bottom illustrate the planes of the cross-sections.

implant after complete drug release (t = 245 d, Fig. 7) confirm the presence of tiny holes (visible as black "circles") in dried samples. The cavities were uniformly distributed throughout the implant, irrespective of the plane of the cross-section. Video 3 shows a series of virtual cross-sections through this implant along the z-axis, starting from the bottom of the cylinder and going to its top (the cartoon in Fig. 7 shows the coordinate system). As it can be seen, the entire implant is depleted from the drug (the few white dots are artefacts), and the inner structure is homogeneous throughout the device. Comparing videos 2 and 3, it seems that the holes (black "circles") created upon drug particle dissolution are somewhat larger and less numerous than the dexamethasone particles initially present in the system (in bright grey). This might be explained by the coalescence of tiny cavities stemming from drug crystal dissolution (polymer chain mobility being non negligible) and/or by artefact creation during sample preparation (drying).

3.3. Implant dimensions and mechanical properties

From a clinical point of view, it is vital that the miniaturised implant placed into the patient's inner ear does not significantly swell upon contact with aqueous body fluids. Otherwise, the surrounding tissue can be harmed, the cochlea being a small and highly sensitive organ. Fig. 10

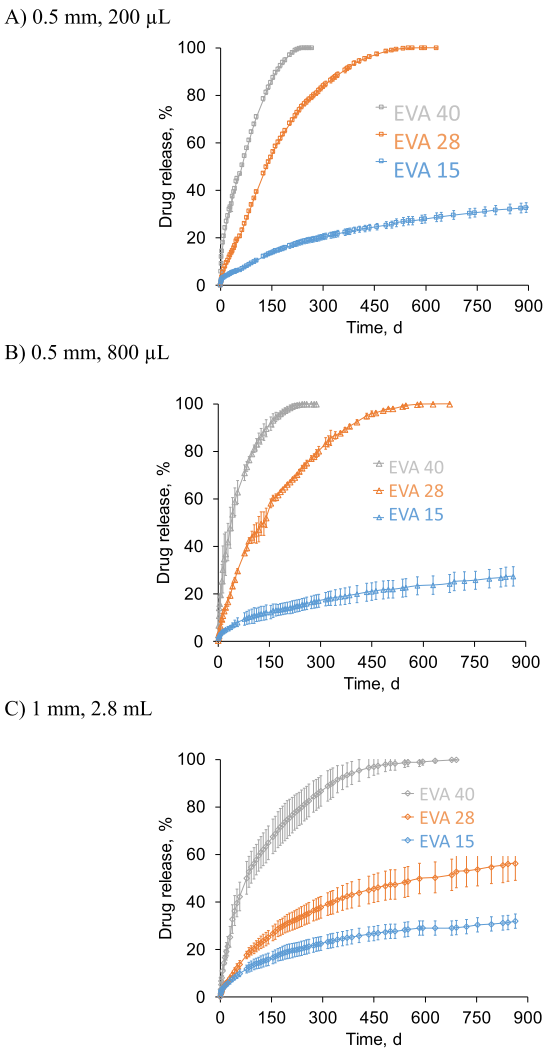

Fig. 8. Dexamethasone release from EVA implants into artificial perilymph at 37 °C. The initial diameter of the implants and volume of the bulk fluids were: A) 0.5 mm & 200 µL, B) 0.5 mm & 800 µL, and C) 1 mm & 2.8 mL. The EVA grades are indicated in the diagrams.

shows the dynamic changes in the diameters of the investigated implants upon exposure to artificial perilymph for up to 300 d at 37 °C. The implants' initial diameter and the release medium volume were: A) 0.5 mm & 200 µL, B) 0.5 mm & 800 µL, and C) 1 mm & 2.8 mL. No noteworthy swelling (or shrinking) was observed, irrespective of the EVA grade, implant diameter and volume of the bulk fluid. This is important for the patient. Note that the implants were not *perfectly round* cylinders and that the implants' diameters were measured by taking optical microscopy pictures, followed by image analysis. Thus, the exact position of the implant when the photo was taken affected the measured diameter to some degree. This can at least partially explain the observed standard deviations and (limited) arbitrary variations.

Another important aspect from a practical (clinical) point of view is the stiffness/flexibility of the miniaturised implants: The surgeon must be able to insert them into the patient's inner ear (and remove empty remnants after drug exhaust, if desired) without harming the surrounding tissue. Thus, the implants must not be too rigid. On the other hand, too-flexible implants are challenging to manipulate and be placed inside the cochlea through a tiny hole drilled into the round window. Hence, appropriate mechanical properties must be provided. A frequently used measure for the elasticity of a material is the "Young modulus", which was determined in this study using the tensile test and a TA.XT plus Texture Analyzer. Fig. 11 shows the results obtained for drug-free and dexamethasone-loaded EVA implants before exposure to the release medium. The values were determined as the slopes of the linear potions of strain-stress plots (0–10% strain). The higher the Young modulus, the stiffer the material. As can be seen, the implants' stiffness increased in the following ranking order: EVA 40 < EVA 28 < EVA 15. This can be explained by the increasing crystallinity of the copolymer with decreasing vinyl acetate content (as discussed above). Furthermore, the addition of the drug (13% *w*/w) led to an increase in the implants' stiffness in EVA 15, but not in the case of EVA 40 and EVA 28. This indicates that (at least at this drug loading) the relatively high elasticity of the pure EVA 40 and EVA 28 regions is dominant. Importantly, the observed mechanical properties of all types of implants can be expected to be appropriate for clinical use.

4. Conclusions

Miniaturised EVA implants show an exciting potential to allow for controlled drug delivery to the inner ear. In contrast to silicone-based devices, the resulting drug release rates are much higher, e.g. complete dexamethasone release can be provided within several months

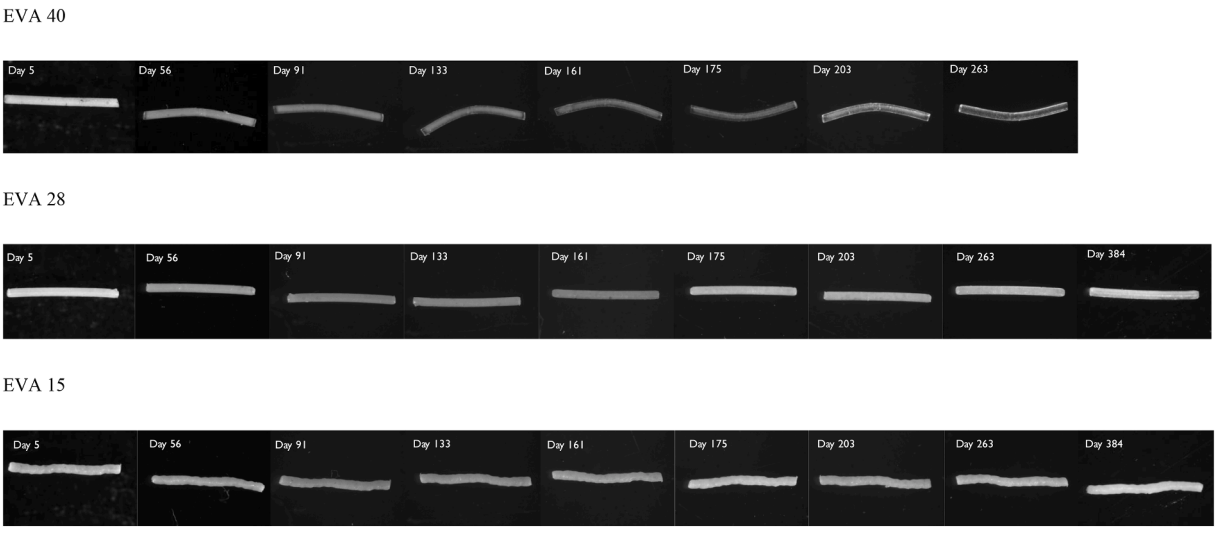

Fig. 9. Optical microscopy pictures of dexamethasone-loaded implants based on EVA 40, EVA 28 and EVA 15 after exposure to artificial perilymph for different periods (as indicated).

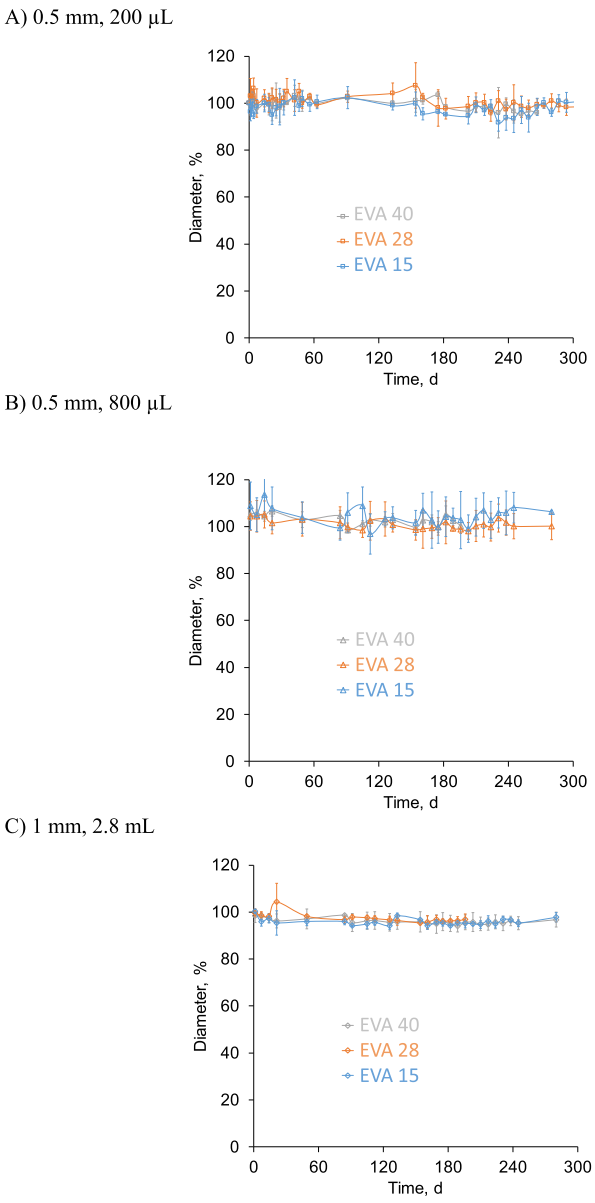

Fig. 10. Dynamic changes in the diameter of EVA implants upon exposure to artificial perilymph at 37 °C. The initial diameter and volume of the bulk fluid were: A) 0.5 mm & 200 µL, B) 0.5 mm & 800 µL, and C) 1 mm & 2.8 mL. The EVA grades are indicated in the diagrams.

compared to many years. Also, the variation of the vinyl acetate content can be used to adjust the release patterns effectively: With increasing vinyl acetate content, the crystallinity of the copolymer decreases, resulting in faster drug diffusion and release. Notably, the systems do not significantly swell and provide appropriate mechanical properties to allow for insertion into the cochlea. This type of implants also offers an interesting potential for the controlled delivery of other types of drugs to the inner ear (e.g. antioxidants) to treat hearing loss and other diseases/ailments of this tiny and highly sensitive organ (e.g. Ménière's disease).

Supplementary data to this article can be found online at https://doi.org/10.1016/j.ijpx.2024.100271.

CRediT authorship contribution statement

Y. Bedulho das Lages: Writing – original draft, Visualization, Validation, Methodology, Investigation, Formal analysis. **N. Milanino:** Investigation. **J. Verin:** Investigation. **J.F. Willart:** Writing – review & editing, Visualization, Validation, Methodology, Investigation, Formal analysis. **F. Danede:** Investigation. **C. Vincent:** Writing – review & editing, Methodology, Conceptualization. **P. Bawuah:** Methodology, Investigation, Formal analysis. **J.A. Zeitler:** Writing – review & editing, Visualization, Validation, Supervision, Resources, Project administration, Methodology, Funding acquisition, Formal analysis. **J. Siepmann:** Writing – review & editing, Visualization, Validation, Supervision, Resources, Project administration, Methodology, Funding acquisition, Formal analysis, Conceptualization.

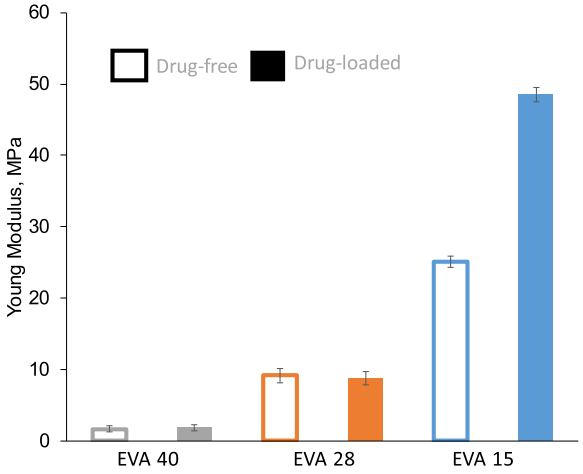

Fig. 11. Young modulus of drug-free and dexamethasone-loaded EVA implants before exposure to the release medium, measured by texture analysis. The EVA grade is indicated on the x-axis.

Declaration of competing interest

The authors declare the following financial interests/personal relationships which may be considered as potential competing interests:

Juergen Siepmann, Axel Zeitler reports financial support was provided by Interreg 2 Seas programme 2014–2020. Juergen Siepmann, Axel Zeitler reports financial support was provided by European Regional Development Fund. Y. Bedulho das Lages, C. Vincent, F. Siepmann, J. Siepmann has patent pending to University of Lille, University Hospital Lille, Inserm. The Editor-in-Chief of the journal is one of the co-authors of this article. The manuscript has been subject to all of the journal's usual procedures, including peer review, which has been handled independently of the Editor-in-Chief. If there are other authors, they declare that they have no known competing financial interests or personal relationships that could have appeared to influence the work reported in this paper.

The Editor-in-Chief of the journal is one of the co-authors of this article. The manuscript has been subject to all of the journal's usual procedures, including peer review, which has been handled independently of the Editor-in-Chief. YBL, CV, FS and JS are listed as inventors of a related patent application: EP23160221.0.

Data availability

Data will be made available on request.

Acknowledgements

This project has received funding from the Interreg 2 Seas programme 2014-2020, co-funded by the European Regional Development Fund under subsidy contract "Site Drug 2S07-033".

References

Arsac, A., Carrot, C., Guillet, J., 2000. Determination of primary relaxation temperatures and melting points of ethylene vinyl acetate copolymers. J. Therm. Anal. Calorim. 61, 681–685.

Baker, R.W., 1987. Controlled Release of Biologically Active Agents. Wiley, New York.

Blasi, P., D'Souza, S.S., Selmin, F., PP, DeLuca, 2005. Plasticizing effect of water on poly (lactide-co-glycolide). J. Control. Release 108, 1–9.

Bode, C., Kranz, H., Fivez, A., Siepmann, F., Siepmann, J., 2019. Often neglected: PLGA/PLA swelling orchestrates drug release: HME implants. J. Control. Release 306, 97–107.

Bourges, J.L., Bloquel, C., Thomas, A., Froussart, F., Bochot, A., Azan, F., et al., 2006. Intraocular implants for extended drug delivery: therapeutic applications. Adv. Drug Deliv. Rev. 58, 1182–1202.

Brogly, M., Nardin, M., Schultz, J., 1997. Effect of vinylacetate content on crystallinity and second-order transitions in ethylene—vinylacetate copolymers. J. Appl. Polym. Sci. 64, 1903–1912.

Brunner, A., Mäder, K., Göpferich, A., 1999. pH and osmotic pressure inside biodegradable microspheres during erosion. Pharm. Res. 16, 847–853.

von Burkersroda, F., Schedl, L., Göpferich, A., 2002. Why degradable polymers undergo surface erosion or bulk erosion. Biomaterials 23, 4221–4231.

Chen, Y.-C., Moseson, D.E., Richard, C.A., Swinney, M.R., Horava, S.D., Oucherif, K.A., et al., 2022. Development of hot-melt extruded drug/polymer matrices for sustained delivery of meloxicam. J. Control Release Off. J. Control Release Soc. 342, 189–200.

Croxatto, H.B., 2000. Clinical profile of Implanon: a single-rod etonogestrel contraceptive implant. Eur. J. Contr. Reprod. Health Care Off. J. Eur. Soc. Contr. 5 (Suppl. 2), 21–28.

El Kechai, N., Agnely, F., Mamelle, E., Nguyen, Y., Ferrary, E., Bochot, A., 2015. Recent advances in local drug delivery to the inner ear. Int. J. Pharm. 494, 83–101.

El Kechai, N., Mamelle, E., Nguyen, Y., Huang, N., Nicolas, V., Chaminade, P., et al., 2016. Hyaluronic acid liposomal gel sustains delivery of a corticoid to the inner ear. J. Control. Release 226, 248–257.

Farhadi, M., Jalessi, M., Salehian, P., Ghavi, F.F., Emamjomeh, H., Mirzadeh, H., et al., 2013. Dexamethasone eluting cochlear implant: histological study in animal model. Cochlear Implants Int. 14, 45–50.

Fredenberg, S., Wahlgren, M., Reslow, M., Axelsson, A., 2011. The mechanisms of drug release in poly(lactic-co-glycolic acid)-based drug delivery systems—a review. Int. J. Pharm. 415, 34–52.

Gao, Z., Schwieger, J., Matin-Mann, F., Behrens, P., Lenarz, T., Scheper, V., 2021. Dexamethasone for inner ear therapy: biocompatibility and bio-efficacy of different dexamethasone formulations in vitro. Biomolecules 11, 1896.

Gausterer, J.C., Saidov, N., Ahmadi, N., Zhu, C., Wirth, M., Reznicek, G., et al., 2020. Intratympanic application of poloxamer 407 hydrogels results in sustained N-acetylcysteine delivery to the inner ear. Eur. J. Pharm. Biopharm. 150, 143–155.

Gehrke, M., Sircoglou, J., Gnansia, D., Tourrel, G., Willart, J.-F., Danede, F., et al., 2016a. Ear Cubes for local controlled drug delivery to the inner ear. Int. J. Pharm. 509, 85–94.

Gehrke, M., Sircoglou, J., Vincent, C., Siepmann, J., Siepmann, F., 2016b. How to adjust dexamethasone mobility in silicone matrices: a quantitative treatment. Eur. J. Pharm. Biopharm. 100, 27–37.

Gehrke, M., Verin, J., Gnansia, D., Tourrel, G., Risoud, M., Vincent, C., et al., 2019. Hybrid ear cubes for local controlled dexamethasone delivery to the inner ear. Eur. J. Pharm. Sci. Off. J. Eur. Fed. Pharm. Sci. 126, 23–32.

Genina, N., Holländer, J., Jukarainen, H., Mäkilä, E., Salonen, J., Sandler, N., 2016. Ethylene vinyl acetate (EVA) as a new drug carrier for 3D printed medical drug delivery devices. Eur. J. Pharm. Sci. 90, 53–63.

Gruber, C.J., 2006. The combined contraceptive vaginal ring (NuvaRing): evaluation of the clinical and pharmacological evidence. Women's Health (Lond. Engl.) 2, 351–356.

Guo, Q., Guo, S., Wang, Z., 2007. Estimation of 5-fluorouracil-loaded ethylene-vinyl acetate stent coating based on percolation thresholds. Int. J. Pharm. 333, 95–102.

Hügl, S., Scheper, V., Gepp, M.M., Lenarz, T., Rau, T.S., Schwieger, J., 2019. Coating stability and insertion forces of an alginate-cell-based drug delivery implant system for the inner ear. J. Mech. Behav. Biomed. Mater. 97, 90–98.

Jaudoin, C., Carré, F., Gehrke, M., Sogaldi, A., Steinmetz, V., Hue, N., et al., 2021a. Transtympanic injection of a liposomal gel loaded with N-acetyl-L-cysteine: a relevant strategy to prevent damage induced by cochlear implantation in guinea pigs? Int. J. Pharm. 604, 120757.

Jaudoin, C., Agnely, F., Nguyen, Y., Ferrary, E., Bochot, A., 2021b. Nanocarriers for drug delivery to the inner ear: Physicochemical key parameters, biodistribution, safety and efficacy. Int. J. Pharm. 592, 120038.

Johnsen, V.U., Nachtrab, G., 1969. Die kristallinität von äthylen-vinylacetat-copolymeren. Angew. Makromol. Chem. 7, 134–146.

Juhn, S.K., Rybak, L.P., Fowlks, W.L., 1982. Transport characteristics of the blood—Perilymph barrier. Am. J. Otolaryngol. 3, 392–396.

Krenzlin, S., Vincent, C., Munzke, L., Gnansia, D., Siepmann, J., Siepmann, F., 2012. Predictability of drug release from cochlear implants. J. Control. Release 159, 60–68.

Kuno, N., Fujii, S., 2011. Recent advances in ocular drug delivery systems. Polymers 3, 193–221.

Le, J., Tsourounis, C., 2001. Implanon: a critical review. Ann. Pharmacother. 35, 329–336.

Lehner, E., Gündel, D., Liebau, A., Plontke, S., Mäder, K., 2019. Intracochlear PLGA based implants for dexamethasone release: challenges and solutions. Int. J. Pharm. X. 1, 100015.

Lehner, E., Liebau, A., Syrowatka, F., Knolle, W., Plontke, S.K., Mäder, K., 2021. Novel biodegradable Round Window Disks for inner ear delivery of dexamethasone. Int. J. Pharm. 594, 120180.

Lehner, E., Menzel, M., Gündel, D., Plontke, S.K., Mäder, K., Klehm, J., et al., 2022. Microimaging of a novel intracochlear drug delivery device in combination with cochlear implants in the human inner ear. Drug Deliv. Transl. Res. 12, 257–266.

Liu, Y., Jolly, C., Braun, S., Janssen, T., Scherer, E., Steinhoff, J., et al., 2015. Effects of a dexamethasone-releasing implant on cochleae: a functional, morphological and pharmacokinetic study. Hear. Res. 327, 89–101.

Liu, Y., Jolly, C., Braun, S., Stark, T., Scherer, E., Plontke, S.K., et al., 2016. In vitro and in vivo pharmacokinetic study of a dexamethasone-releasing silicone for cochlear implants. Eur. Arch. Oto-Rhino-Laryngol. Off. J. Eur. Fed. Oto-Rhino-Laryngol. Soc. EUFOS Affil. Ger. Soc. Oto-Rhino-Laryngol. - Head Neck Surg. 273, 1745–1753.

Mäder, K., Lehner, E., Liebau, A., Plontke, S.K., 2018. Controlled drug release to the inner ear: co12ncepts, materials, mechanisms, and performance. Hear. Res. 368, 49–66.

Mansour, D., 2010. Nexplanon(®): what Implanon(®) did next. J. Fam. Plann. Reprod. Health Care 36, 187–189.

Moroni, S., Bischi, F., Aluigi, A., Campana, R., Tiboni, M., Casettari, L., 2023. 3D printing fabrication of Ethylene-Vinyl Acetate (EVA) based intravaginal rings for antifungal therapy. J. Drug Deliv. Sci. Technol. 84, 104469.

Novák, A., de la Loge, C., Abetz, L., van der Meulen, E.A., 2003. The combined contraceptive vaginal ring, NuvaRing: an international study of user acceptability. Contraception 67, 187–194.

Oliveira, P.F.M., Willart, J.-F., Siepmann, J., Siepmann, F., Descamps, M., 2018. Using milling to explore physical states: the amorphous and polymorphic forms of dexamethasone. Cryst. Growth Des. 18, 1748–1757.

O'Neil, M.J. (Ed.), 2001. The Merck Index: An Encyclopedia of Chemicals, Drugs, and Biologicals, 13th ed. Merck, Whitehouse Station, N.J.

Qnouch, A., Solarczyk, V., Verin, J., Tourrel, G., Stahl, P., Danede, F., et al., 2021. Dexamethasone-loaded cochlear implants: How to provide a desired "burst release.". Int. J. Pharm. X. 3, 100088.

Reinhard, C.S., Radomsky, M.L., Saltzman, W.M., Hilton, J., Brem, H., 1991. Polymeric controlled release of dexamethasone in normal rat brain. J. Control. Release 16, 331–339.

Rongthong, T., Qnouch, A., Gehrke, M.M., Danede, F., Willart, J.F., de Oliveira, P.F.M., et al., 2022. Long term behavior of dexamethasone-loaded cochlear implants: in vitro & in vivo. Int. J. Pharm. X. 4, 100141.

Salem, H., Baskin, S.I. (Eds.), 1993. New Technologies and Concepts for Reducing Drug Toxicities. CRC, Boca Raton, FL.

Salyer, I.O., Kenyon, A.S., 1971. Structure and property relationships in ethylene–vinyl acetate copolymers. J. Polym. Sci. [A1] 9, 3083–3103.

Schädlich, A., Kempe, S., Mäder, K., 2014. Non-invasive in vivo characterization of microclimate pH inside in situ forming PLGA implants using multispectral fluorescence imaging. J. Control. Release 179, 52–62.

Schneider, C., Langer, R., Loveday, D., Hair, D., 2017. Applications of ethylene vinyl acetate copolymers (EVA) in drug delivery systems. J. Control. Release 262, 284–295.

Siepmann, J., Siepmann, F., 2012. Modeling of diffusion controlled drug delivery. J. Control. Release 161, 351–362.

Siepmann, J., Siepmann, F., 2013. Mathematical modeling of drug dissolution. Int. J. Pharm. 453, 12–24.

Siepmann, J., Siepmann, F., 2020. Sink conditions do not guarantee the absence of saturation effects. Int. J. Pharm. 577, 119009.

Swan, E.E.L., Mescher, M.J., Sewell, W.F., Tao, S.L., Borenstein, J.T., 2008. Inner ear drug delivery for auditory applications. Adv. Drug Deliv. Rev. 60, 1583–1599.

Toulemonde, P., Risoud, M., Lemesre, P.E., Tardivel, M., Siepmann, J., Vincent, C., 2022. 3D analysis of gerbil cochlea with cochlear implant. Eur. Ann. Otorhinolaryngol. Head Neck Dis. 139, 333–336.

Wang, L., Fang, P., Ye, C., Feng, J., 2006. Solid-state NMR characterizations on phase structures and molecular dynamics of poly(ethylene-co-vinyl acetate). J. Polym. Sci. Part B Polym. Phys. 44, 2864–2879.

Wilk, M., Hessler, R., Mugridge, K., Jolly, C., Fehr, M., Lenarz, T., et al., 2016. Impedance changes and fibrous tissue growth after cochlear implantation are correlated and can be reduced using a dexamethasone eluting electrode. Yamamoto M, editor. PLoS One 11, e0147552.

World Health Organization, 2021. World Report on Hearing [Internet]. [cited 2023 May 15]. Available from: https://www.who.int/teams/noncommunicable-diseases/sensory-functions-disability-and-rehabilitation/highlighting-priorities-for-ear-and-hearing-care.

Zhang, Q., Lin, W., Yang, G., Chen, Q., 2002. Studies on the phase structure of ethylene-vinyl acetate copolymers by solid-state1H and13C NMR. J. Polym. Sci. Part B Polym. Phys. 40, 2199–2207.